STABILIZATION OF A HIGH PRESSURE JET FLAME WITH HEAT LOSSES BY LES

P. Gruhlke*, H. Janbazi*, I. Wlokas*, C. Beck, A. M. Kempf***

pascal.gruhlke@uni-due.de

*Chair of Fluid Dynamics, Institute for Combustion and Gasdynamics (IVG), University of Duisburg-Essen, Carl-Benz-Straße 199, 47057 Duisburg, Germany

**Siemens AG, Mellinghofer Straße 55, 45473 Mülheim an der Ruhr, Germany

Abstract

Large-eddy simulations (LES) of a lean preheated high pressure jet flame are presented, comparing a premixed flamelet generated manifolds (PFGM) and a finite rate chemistry (FRC) approach, with dynamic flame thickening in either case. The impact of the combustion models on the stabilization of the flame is investigated. The PFGM tables are calculated from the detailed GRI 3.0 reaction mechanism. For the FRC combustion model, both a compact skeletal mechanism and the DRM19 mechanism extended by an OH* sub-mechanism have been tested. In the simulations, heat losses due to chamber cooling are considered by estimating and applying isothermal wall temperatures. The significant flame lift was predicted by the FRC and PFGM combustion models applying non-adiabatic boundary conditions. Simulation results of the flame stabilization improved using the DRM19 reaction mechanism. The correlation of heat release and OH* species was found to be insufficient in the present case for comparing flame lift-off monitored by OH* to flame lift-off determined by heat-release.

Introduction

Incomplete CO burnout becomes critical at gas turbine part-load operation. At the same time, more efficient baseload operation requires increasing combustor outlet temperature, potentially increasing NO_x emissions. Large-eddy simulations have proven to be suitable for combustion chamber development. For the investigation of the CO and NO_x pollutant formation, numerous methods have been used to model combustion [1,2] including the artificial flame thickening approach (ATF) [3,4]. In the FRC approach, the reaction progress is solved during runtime and combustion kinetics are directly considered. In the PFGM method, chemistry is tabulated from adiabatic 1-D premixed flames prior to the simulations and looked up during runtime based on control variables. This approach reduces the computational cost in comparison to direct chemistry, while additional effects such as strain or heat losses need to be modelled [5]. Large-eddy simulations coupled with ATF have proven to be a promising method with both finite rate chemistry [3,6] and premixed flamelet generated manifolds (PFGM) [4,5]. A reliable prediction of CO and NO_x necessitates the correct description of the flow field, flame shape and stabilization. A challenge for numerical modelling is presented by

lifted flames, where the stabilization is affected by different mechanisms such as quenching, auto-ignition delay [7,8] or high reactant flow rates [6]. In a new lean preheated high pressure jet flame examined by Lammel, Severin, Ax and co-workers [9,10], heat losses were found to have an impact on the flame stabilization at baseload operation as OH*-chemiluminescence indicated a lifted burning flame.
In the present work, FRC and PFGM and different reaction mechanisms are applied and their impact on the prediction of the flame stabilization is investigated.

Modelling Approach

With FRC, the laminar and turbulent Prandtl and Schmidt numbers are 0.7 and a unity Lewis assumption is made. Sutherland's law for air determines the transport properties. Favre-filtered transport equations are solved for the mixture fraction, absolute total enthalpy and species. To keep computational costs low, a skeletal mechanism has been developed for the limited range of conditions studied in this work. The mechanism was developed from the H_2/O_2 branch of the C1 mechanism by Li et al. [11], the CH_4/O_2 branch of the methane combustion mechanism by Cremer [12], and the C/N/O branch of GRI 3.0 [13]. Thermodynamic and transport properties were taken from GRI 3.0. A genetic algorithm [14,15] was used for the reduction and optimization, where GRI 3.0 was used as a reference. Optimization targets were the laminar flame speed, temperature and CO and NO_x species, potentially allowing for pollutant predictions in future studies. The new reaction mechanism includes 20 species and 35 reactions. The validation against GRI 3.0 indicated very good agreement for the limited operational range the mechanism has been developed for. In order to examine the skeletal mechanism's quality and applicability, the more detailed and established reaction mechanism DRM19 [16] was used and extended by an 11-step sub-mechanism [17] to include OH* species for direct comparison against experimental data.
The PFGM combustion model has been implemented by Dederichs et al. [18] and Mahiques et al. [19]. Prior to simulations, look-up tables are generated from 1-D laminar, premixed, freely propagating flames using Cantera with GRI 3.0. Control variables for table access are the mixture fraction Z and enthalpy h_t and the normalized progress variable c. The latter is defined as $c = Y_{CO_2}(\tilde{Z}, \tilde{h}_t)/Y_{CO_2}^{max}(\tilde{Z}, \tilde{h}_t)$ and is determined from the CO_2 mass fraction Y_{CO_2} and $Y_{CO_2}^{max}$ at equilibrium for a given mixture fraction and enthalpy. Favre-filtered transport equations are solved for the mixture fraction, absolute total enthalpy and progress variable. Heat losses are considered in the PFGM table generation by calculating flamelets at different enthalpy levels. This is achieved by lowered fresh gas temperatures.
In order to resolve the thin flame front on the numerical grid, an artificial flame thickening (ATF) approach is used, following Dederichs et al. [18]. Thickening is applied to the species transport equation for FRC and to the progress variable transport equation in PFGM. Unphysical thickening outside the flame region is avoided by applying a flame sensor. The thickening of the flame reduces the

wrinkling of the flame, which is compensated by applying the modified Charlette model [20].

Experiments and numerical setup

The chamber geometry and the inlet conditions are shown in Fig. 1. The lean partially-premixed CH_4-air mixture at 8 bar enters the combustion chamber with a jet Reynolds number of $6 \cdot 10^5$ and a bulk velocity of 120 m/s. The turbulent fluctuations and integral length-scale are approximately 10 m/s and 2.8 mm. Laser measurement techniques were applied in the experiments as the chamber is optically accessible and the flame shape and stabilization has been determined from OH* chemiluminescence (OH*-CL). More details on the experiments can be found in the work of Lammel, Severin, Ax and co-workers [9,10]. The combustor quartz glass walls were cooled in the experiments causing severe heat losses to the flame. We calculated heat transfer coefficients using coolant mass flows and temperatures (Lammel and Ax, personal communication, July 2016) and LES data. The estimations confirmed a burner baseplate temperature of 600 K [10] and temperatures of {920, 1000, 980, 960} K in the zones of {0−0.1, 0.1−0.2, 0.2−0.4, 0.4−0.84} m within the chamber.

The LES was performed using OpenFOAM. The temporal discretization blends explicit and implicit contributions, weighted at 0.3 and 0.7, with a convective CFL number of 0.3. Convection is discretized by a TVD scheme, it should be kept in mind that such schemes are more dissipative than one would wish for LES. The mesh consists of 8.1M hexahedral cells with 1.0 mm cell size in the flame region.

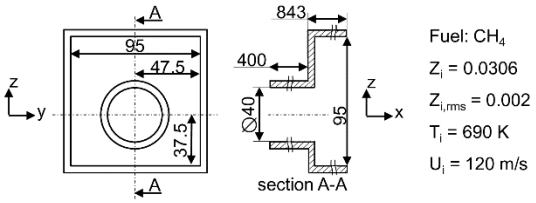

Figure 1. Chamber geometry and inlet conditions.

Results

In the experiments, OH*-CL has been used as an indicator for the flame heat release and thus to determine the flame shape and stabilization. It has been shown that the flame tends to burn asymmetrically and lifted as presented in Fig. 2a. The line-averaged (in z-direction) mean carbon dioxide source term from PFGM, the mean reaction heat release from FRC and the mean OH* mass fractions from FRC simulations applying the extended DRM19 mechanism are used for comparison against the experimentally obtained OH*-CL. These quantities are closely related and often used to compare chemiluminescence images from experiments to simulation results. In the experiments, a flame lift is observed at the upper side of the chamber which intensifies at the lower side. The PFGM model with chemistry tabulated from GRI 3.0 (Fig. 2b) and the FRC model with the new skeletal reaction

mechanism (Fig. 2c) show a qualitatively similar flame shape and lift-off. Figure 2d presents the mean OH* mass fraction from FRC simulations with DRM19 which shows very good agreement with the experimentally determined OH*-CL. The prediction of the asymmetric flame shape is significantly improved, and the lift-off height is in better agreement with the experiments.

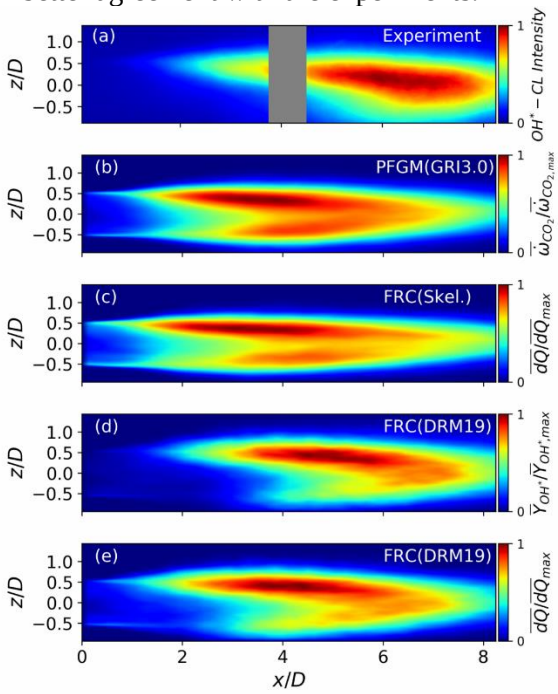

Figure 2. Line-averaged (in z-direction) mean normalized experimental OH*-CL a), CO_2 source term from PFGM b), reaction heat release rate from FRC using the skeletal mechanism c), OH* mass fraction for FRC using DRM19 mechanism d) and reaction heat release rate from FRC using DRM19 mechanism e).

The reaction heat release rate based on DRM19 (Fig. 2e) indicates lower heat release at the lower side of the chamber in comparison to PFGM and the FRC with the skeletal mechanism. Furthermore, local heat release rates of around 50% at the lower side of the chamber are observed for PFGM and FRC simulations using the skeletal mechanism, while only around 20% are identified from simulations applying DRM19. PFGM results might improve by considering strain effects which are not accounted for yet. Discrepancies from simulations using the skeletal mechanism in the prediction of the flame stabilization might be attributed to shortcomings in the choice of optimization targets while mechanism development. The identification of species and reactions which are significant for the prediction of the flame stabilization in a non-adiabatic environment may improve the mechanism. Deviations between the mean Y_{OH^*} and heat release rate are identified comparing Figs. 2d and 2e. The heat release rate indicates a similar flame shape as

OH* while a smaller lift-off height is observed. Interestingly, reduced but still considerable large heat release rates are found at x/D<3, which indicates that the flame is not fully lifted as suggested by the OH* mass fraction. This confirms that OH* is not an adequate indicator of local extinction [21] and is only partially agreeing with work that considers OH* a direct marker for the heat release rate.

Conclusion

Large-eddy simulations of the flame stabilization in a pressurized jet flame have been performed and different combustion models and reaction mechanisms were compared. An asymmetric and lifted flame was observed in the experiments which was also predicted by PFGM and FRC. Simulation results with an extended DRM19 reaction mechanism including OH* species were directly compared to the experimentally observed OH* chemiluminescence and showed very good agreement. The correlation of heat release and OH* species was shown to be insufficient for the present study as a distinct flame lift was found for the OH* species mass fraction while reduced but significant heat release rates were observed.

References

[1] Jella S., Gauthier, P., Bourque, G., Berthorson, J., Bulat, G., Rogerson, J., Sadasivuni, "Large Eddy Simulations of a Pressurized, Partially-Premixed Swirling Flame With Finite-Rate Chemistry", *ASME Turbo Expo* (2017).

[2] Bulat, G., Jones, W. P., & Marquis, A. J., "NO and CO formation in an industrial gas-turbine combustion chamber using LES with the Eulerian sub-grid PDF method", *Combust. Flame*, 161(7), 1804-1825 (2014).

[3] Schmitt, P., Poinsot, T., Schuermans, B., & Geigle, K. P., "Large-eddy simulation and experimental study of heat transfer, nitric oxide emissions and combustion instability in a swirled turbulent high-pressure burner", *J. Fluid Mech.*, 570, 17-46 (2007).

[4] Gruhlke, P., Proch, F., Kempf, A. M., Mahiques, E. I., Dederichs, S., & Beck, C., "Prediction of CO and NOx Pollutants in a Stratified Bluff Body Burner", *ASME Turbo Expo* (2017).

[5] Proch, F., & Kempf, A. M., "Modeling heat loss effects in the large eddy simulation of a model gas turbine combustor with premixed flamelet generated manifolds", *Proc. Comb. Inst.*, 35(3), 3337-3345 (2015).

[6] Legier, J. P., Poinsot, T., & Veynante, D, "Dynamically thickened flame LES model for premixed and non-premixed turbulent combustion", *Proc. of the summer program*, pp. 157-168 (2000).

[7] Cabra, R., Myhrvold, T., Chen, J. Y., Dibble, R. W., Karpetis, A. N., & Barlow, R. S., "Simultaneous laser Raman-Rayleigh-LIF measurements and numerical modeling results of a lifted turbulent H2/N2 jet flame in a vitiated coflow", *Proc. Comb. Inst.*, 29(2), 1881-1888 (2002).

[8] Domingo, P., Vervisch, L., & Veynante, D., "Large-eddy simulation of a

lifted methane jet flame in a vitiated coflow", *Combust. Flame*, 152(3), 415-432 (2008).

[9] Lammel, O. et al.,"High Momentum Jet Flames at Elevated Pressure: A—Experimental and Numerical Investigation for Different Fuels", *ASME Turbo Expo* (2017).

[10] Severin, M., et al. "High Momentum Jet Flames at Elevated Pressure: B—Detailed Investigation of Flame Stabilization With Simultaneous PIV and OH-LIF", *ASME Turbo Expo* (2017).

[11] Li, J., Zhao, Z., Kazakov, A., Chaos, M., Dryer, F. L., & Scire, J. J., "A comprehensive kinetic mechanism for CO, CH2O, and CH3OH combustion", *Int. J. Chem. Kin.*, 39(3), 109-136 (2007).

[12] Cremer, H., „Zur Reaktionskinetik der Methan- Oxidation", *Chemie-Ing.Technik*, 44(1- 2), 8-15 (1972).

[13] Smith, G. P. et al. *http://www.me.berkeley.edu/gri_mech/* (2000).

[14] Sikalo, N., Hasemann, O., Schulz, C., Kempf, A., & Wlokas, I., "A Genetic Algorithm- Based Method for the Automatic Reduction of Reaction Mechanisms", *Int. J. Chem. Kin.*, 46(1), 41-59 (2014).

[15] Sikalo, N., Hasemann, O., Schulz, C., Kempf, A., & Wlokas, I., "A Genetic Algorithm–Based Method for the Optimization of Reduced Kinetics Mechanisms", *Int. J. Chem. Kin.*, 47(11), 695-723 (2015).

[16] Kazakov, Andrei, and Michael Frenklach. "Reduced reaction sets based on GRI-Mech 1.2.", *http://www.me.berkeley.edu/drm* (1994).

[17] Kathrotia, T., Riedel, U., Seipel, A., Moshammer, K., & Brockhinke, A., "Experimental and numerical study of chemiluminescent species in low-pressure flames", *Applied Physics B*, 107(3), 571-584 (2012).

[18] Dederichs, S., Zarzalis, N., & Beck, C., "Validation of a novel LES approach using tabulated chemistry for thermoacoustic instability prediction in gas turbines", *ASME Turbo Expo* (2015).

[19] Mahiques, E. I., Dederichs, S., Beck, C., Kaufmann, P., & Kok, J. B. W., "Coupling multicomponent droplet evaporation and tabulated chemistry combustion models for large-eddy simulations", *Int. J. Heat Mass Transfer*, 104, 51-70 (2017).

[20] Wang, G., Boileau, M., & Veynante, D., "Implementation of a dynamic thickened flame model for large eddy simulations of turbulent premixed combustion", *Combust. Flame*, 158(11), 2199-2213 (2011).

[21] Najm, H. N., Paul, P. H., Mueller, C. J., & Wyckoff, P. S., "On the adequacy of certain experimental observables as measurements of flame burning rate", *Combust. Flame*, 113(3), 312-332 (1998).